Magnetic relaxation of mesoscopic molecules

1998 J. Phys.: Condens. Matter 10 10075

(http://iopscience.iop.org/0953-8984/10/44/014)

J. Phys.: Condens. Matter **10** (1998) 10075–10099. Printed in the UK PII: S0953-8984(98)94232-1

Magnetic relaxation of mesoscopic molecules

Alois Würger†

Institut Laue–Langevin, Avenue des Martyrs, BP 156, 38042 Grenoble Cédex 09, France

Received 18 May 1998, in final form 11 August 1998

Abstract. The relaxation dynamics of nanoscale molecules such as $Mn_{12}Ac$ arises from spin–lattice coupling and interaction with nuclear spins. Using a resolvent method in terms of the energy eigenstates and the first Born approximation with respect to phonon scattering, and averaging over the hyperfine field, we obtain a controlled approximation for the non-equilibrium magnetic relaxation behaviour and, in particular, for the corresponding rate. The rate is finite at $T = 0$, then increases linearly with T, and shows Arrhenius behaviour at higher temperature; for zero magnetic field B there are two different activation energies. The resonances as a function of B are shown to be slightly asymmetric about $B = 0$. Taking account of a quartic crystal field gives rise to a temperature-dependent shift of the resonant values of B. We find that, contrary to previous results, the rate is independent of the magnetic field at low but finite temperatures; for $T \to 0$ it is linear in B. Finally we compare our findings with various experimental data.

1. Introduction

During the last decade, nanoscale molecules have attracted much attention because of their particular long-time magnetic relaxation behaviour. These systems are interesting from a fundamental point of view, as possible realizations for macroscopic quantum coherence (cf. Leggett's contribution to reference [1]), and since they permit one to study dissipation mechanisms in magnets of mesoscopic size that might be relevant for the dynamics of domain walls in bulk materials [2, 3].

These molecules comprise a few tens of atoms whose electronic spins couple to a total spin S; for $Mn_{12}Ac$ one has $S = 10$. A uniaxial crystal field gives rise to an energy ladder with degenerate ground states $S_z = \pm S$, and residual couplings result in a tiny ground-state splitting Ω. Calculating Ω is not a simple matter; it has been tackled in a semiclassical approximation, i.e. $S \to \infty$ with $\hbar S$ constant, and by path integral methods for quantum spins [4–7]; for recent reviews see references [8, 1].

Various experiments have revealed a rich dependence of the relaxation behaviour on temperature and magnetic field. The rate shows activated behaviour above a few K [9–13], whereas it tends towards a constant at lower T [10, 11]; the characteristic timescale may reach several weeks. As a function of the magnetic field, the rate shows maxima at certain values B_J [12–16]; see (1.2) below.

The observed relaxation behaviour indicates the relevance of other degrees of freedom. Coupling to elastic waves, or phonons, is needed to ensure energy conservation both for transitions between the ground states [17, 18] and from excited levels [19–23]. The hyperfine interaction couples electronic and nuclear spins; it gives rise to a random magnetic field and influences the relaxation dynamics [24–26].

† Present address: Université Bordeaux-I, CPMOH, 351 cours de la Libération, 33405 Talence, France.

0953-8984/98/4410075+25$19.50

The present theory applies quite generally to an easy-axis magnet with spin S. More specifically, we consider a $Mn_{12}Ac$ molecule that consists of eight Mn^{3+} ions with spin 2 and four Mn^{4+} ions with spin $\frac{3}{2}$ [1, 26]. The magnetic interaction leads to a total spin $S = 10$, and the tetragonal molecular symmetry defines an 'easy axis' or quantization direction S_z. The resulting 21 states are split by a quadratic spin anisotropy $-AS_z^2$; an external magnetic field along the z-axis adds a Zeeman term $-g\mu BS_z$, thus giving rise to the levels

$$E_M = -AM^2 - g\mu BM \tag{1.1}$$

where the magnetic quantum number M denotes the eigenvalues of S_z. The anisotropy parameter takes a value of $A/k_B \approx 0.6$ K.

For $B = 0$, the states $|M\rangle$ and $|-M\rangle$ are degenerate. Similar pairs of resonant levels $|-M\rangle$ and $|M - J\rangle$ occur at

$$B_J = J\frac{A}{g\mu} \tag{1.2}$$

where we have $E_{-M} = E_{M-J}$.

Whereas the energy levels of the molecule are well described in terms of the static crystal field, the dynamics, i.e., the magnetic relaxation, requires one to take into account bath variables. Coupling to nuclear spins, i.e. the hyperfine interaction, has been considered in detail in references [25, 26]. Since there is no simple expression for the microscopic coupling potential in terms of the collective electron spin $\boldsymbol{S}$, we subsume the hyperfine interaction in an additional magnetic field energy

$$E_{\rm hf} = -h_xS_x - h_zS_z \tag{1.3}$$

where the field components h_x and h_z are random quantities, with distribution laws $P_i(h_i)$.

Thus the spin Hamiltonian comprises anisotropy and Zeeman terms (1.1), and the hyperfine interaction (1.3),

$$H_{\rm S} = -AS_z^2 - g\mu BS_z - \boldsymbol{h}\cdot\boldsymbol{S}. \tag{1.4}$$

The transverse field h_x is of little consequence for the energy levels, but it mixes the angular momentum states and is therefore essential for the dynamics. In accordance with the estimation given in [26], we will assume the fields h_i to be small as compared to A.

At first sight the longitudinal hyperfine field h_z would seem to be of little relevance; it merely causes a slight energy shift that is smaller than the separation $(2M+1)A$ of adjacent levels M and $M+1$. Since, depending on the nuclear spin state, the hyperfine coupling changes from one spin angular momentum (M) to another (M'), in (1.4) we assume that it is linear in the difference $M - M'$. Since the actual nuclear spin state consists of a superposition of different one-atom states, we may treat the h_z as a random variable.

We will see that the nuclear spins play the role of a magnetization reservoir, since they change, through the transverse coupling S_xh_x, the magnetic state of the molecule. They do not, however, permit energy relaxation, since their level spacings are much smaller than those of the electron spin, i.e., there is no resonant spin-flip interaction between nuclear and electron spins.

Relaxation requires contact to a heat bath; this is provided by coupling to the elastic waves of the host crystal,

$$V = v(\boldsymbol{S})\sum_s \gamma_s\varepsilon_s \tag{1.5}$$

where s labels the three acoustic phonon branches with coupling energy γ_s and the corresponding strain field

$$\varepsilon_s = \sum_{\boldsymbol{q}} \left(\hbar/2NM\omega_{\boldsymbol{q}s}\right)^{1/2} q\left(\mathrm{i}b_{\boldsymbol{q}s} - \mathrm{i}b_{\boldsymbol{q}s}^\dagger\right). \tag{1.6}$$

The factor q arises for quantized acoustic modes, $[b^\dagger_{qs}, b_{q's'}] = \delta_{qq'}\delta_{ss'}$, with wavelengths larger than the size of the molecule. Because of time-reversal symmetry, $v(\boldsymbol{S})$ must be of even order in the spin operators. According to the discussion in [26], the most important term reads

$$v(\boldsymbol{S}) = S_x S_z + S_z S_x. \tag{1.7}$$

In this paper we will use two types of spin state, namely the eigenstates of S_z and those of H_S [17]. The former are labelled by capital letters, $|M\rangle$, with $-S \leqslant M \leqslant S$; they fulfil $S_z|M\rangle = M|M\rangle$. The energy eigenstates $|n\rangle$ are defined by $H_S|m\rangle = E_m|m\rangle$. We will use a notation such that there is a close correspondence between the states $|M\rangle$ and $|m\rangle$ with $m = M$.

Very recently, the relaxation behaviour arising from phonon coupling has been studied perturbatively in the angular momentum basis [21–23], with emphasis on the transition between quantum and thermally activated regimes. Luis *et al* [22] considered both hyperfine (or dipolar) interactions (1.7) and a transverse crystal field, and they investigated the effect of the resonances at B_J on the relaxation rate and the hysteresis behaviour.

Contrary to that of references [21, 23], our approach is based on the energy eigenstates of the spin system. One aspect of this choice will be discussed below equation (8.2). We study in detail the relevant diagrams of the perturbation theory, and we present novel results concerning the direct process that is predominant at very low T, in particular the magnetic field dependence of the relaxation rate.

We close this introductory section with an outline of the paper. Sections 2 and 3 provide the formal apparatus for calculating the time evolution of the electron spin system; after setting up a perturbation theory in terms of the spin–phonon coupling, we evaluate the rate matrix and the resulting stationary state, and consider the time dependence of the magnetization.

In the remaining sections, we apply this theory to the $Mn_{12}Ac$ molecule, and discuss the dynamics of the magnetization. Sections 4 and 5 contain an approximate evaluation of the energy eigenstates and the corresponding transition rates. In section 6 we perform the averaging over the longitudinal hyperfine field and derive the rates explicitly; the temperature and field dependencies of the rate are addressed in section 7 and compared with experimental findings. In sections 8 and 9 we discuss and summarize our results.

2. Time evolution

In terms of the statistical operator, the time evolution of the system is determined by

$$\hat{\rho}(t) = \mathrm{e}^{-\mathrm{i}Ht/\hbar}\hat{\rho}\mathrm{e}^{\mathrm{i}Ht/\hbar} \equiv \mathrm{e}^{-\mathrm{i}\mathcal{L}t}\hat{\rho}. \tag{2.1}$$

In the second equality, we have introduced the Liouville operator $\mathcal{L}$ whose action is given by von Neumann's equation $\hbar\mathcal{L}\hat{\rho} \equiv [H, \hat{\rho}]$. Here, the Hamiltonian

$$H = H_0 + V = H_S + H_B + V$$

comprises the spin part (1.4), the coupling term (1.5), and the energy of the uncoupled phonon bath

$$H_B = \sum_{qs} \hbar\omega_{qs} b^\dagger_{qs} b_{qs}.$$

2.1. Perturbation theory

Our evaluation of the spin dynamics is based on standard weak-coupling theory. We assume that the statistical operator factorizes at the initial time, and we treat the spin–phonon coupling perturbatively. The factorization property permits us to define the reduced time evolution operator

$$\mathcal{U}(t) = \langle \mathrm{e}^{\mathrm{i}\mathcal{L}t} \rangle \tag{2.2}$$

where the angular brackets $\langle \cdots \rangle = \mathrm{tr}_{\mathrm{B}}(\cdots \rho_{\mathrm{B}})$ denote the partial trace over the bath degrees of freedom. The average over spin variables with weight ρ will be denoted by $\langle \cdots \rangle_\rho = \mathrm{tr}(\cdots \rho)$.

After taking the Laplace transform of (2.2), the propagator can be written in resolvent form:

$$\mathcal{U}(z) = -[z + \Lambda + \Sigma(z)]^{-1} \tag{2.3}$$

where Λ describes the time evolution in the absence of phonon coupling. The self-energy Σ can be obtained by applying a projection operator technique [27–29], or by performing an appropriate cumulant expansion of $\mathcal{U}(t)$ in terms of $\mathcal{L}_V$. Truncating the perturbation series at second order, we find

$$\Sigma(t) = \langle \mathcal{L}_V \mathrm{e}^{-\mathrm{i}\mathcal{L}_0 t} \mathcal{L}_V \rangle. \tag{2.4}$$

The 'superoperators' $\mathcal{U}$, Λ, Σ, act on the spin degrees of freedom only. From the 21 spin states $|M\rangle$, one may construct 21^2 linearly independent spin operators S_α, $S_\alpha S_\beta$, etc. A more convenient description, however, is provided by the standard basis operators

$$X_{nm} \equiv |n\rangle\langle m|. \tag{2.5}$$

Expanding the spin state in terms of X_{nm}, we find

$$\rho = \sum_{nm} \rho_{nm} X_{nm} \tag{2.6}$$

with $\rho_{nm} = \rho^*_{mn}$, positive ρ_{nn}, and $\mathrm{tr}(\rho) = 1$.

Since $\mathcal{U}$, Λ, and Σ are linear operators on the space spanned by $\{X_{nm}\}$, they are represented by tetrads with $21^2 \times 21^2 = 21^4$ entries:

$$\mathcal{U}_{nmpq}(t) = \mathrm{tr}(X^\dagger_{nm} \mathcal{U}(t) X_{pq}) \tag{2.7}$$

etc. The matrix representation is significantly simplified by the fact that the frequency tetrad $\Lambda_{nmn'm'} = \Delta_{nm}\delta_{nn'}\delta_{mm'}$ is diagonal in the basis X_{nm}. Here, we have defined the resonance frequency

$$\Delta_{nm} = (E_n - E_m)/\hbar \tag{2.8}$$

for transition between levels n and m. Because of the level repulsion due to the transverse field, Δ_{nm} cannot be zero, but always takes a finite value.

In order to evaluate the self-energy, we use $\hbar\mathcal{L}_V * = [V, *]$ in (2.4) and thus obtain the well-known double commutator

$$\Sigma_{nmpq}(t) = \frac{1}{\hbar^2}\mathrm{tr}\Big\{ X^\dagger_{nm}\Big[V, \mathrm{e}^{-\mathrm{i}H_0 t/\hbar}\big[V, X_{pq}\rho_{\mathrm{B}}\big]\mathrm{e}^{\mathrm{i}H_0 t/\hbar}\Big]\Big\} \tag{2.9}$$

where $\mathrm{tr}\{\cdots\}$ denotes the trace over both spin and bath variables. Note that the weight is given by the bath equilibrium density ρ_{B} only.

Equations (2.4)–(2.9) summarize the perturbation theory for the dynamics of a few 'system' degrees of freedom coupled to a phonon heat bath. For a detailed discussion, the reader is referred to Haake's book, reference [29]; results similar to (2.9) have been derived

for the dissipative dynamics of rotational tunnelling [30], the spin–phonon model [31], and various other systems.

Now we turn to the self-energy (2.9). Evaluating the double commutator and inserting the phonon coupling potential $V = \sum_{nm} V_{nm} X_{nm}$ gives rise to a variety of terms. Yet it turns out that the random phases of the V_{nm} impose severe selection rules. The spin operators in (1.7) involve the spin–orbit coupling on each Mn ion. Accordingly, the phase of the matrix element $V_{nm} = \langle n|V|m\rangle$ arises from the superposition of phases for each ion and each phonon mode.

Hence V_{nm} may be treated as a complex number with a random phase, resulting in the relation

$$\langle V_{nm} V_{pq}\rangle = \langle |V_{nm}|^2\rangle \delta_{nq}\delta_{mp} \tag{2.10}$$

which, in turn, restricts the number of finite entries of (2.9) according to

$$\Sigma_{nmpq} = \Sigma_{nmnm}\delta_{np}\delta_{mq} + \Sigma_{nnpp}\delta_{nm}\delta_{pq} \tag{2.11}$$

and greatly simplifies the subsequent analysis.

Due to the selection rules on Λ_{nmpq} and Σ_{nmpq}, the propagator matrix $\mathcal{U}_{nmpq}$ is block-diagonal. Time evolution of the off-diagonal operators X_{nm}, with $n \neq m$, completely factorizes, i.e., there are $2S \times (2S+1)$ one-dimensional blocks $\mathcal{W}_{nmnm}$ whose self-energy involves the first term on the r.h.s. of (2.11). The second term mixes all projections $X_{nn} = |n\rangle\langle n|$ and results in a larger block

$$\mathcal{V}_{nm} \equiv \mathcal{U}_{nnmm} \tag{2.12}$$

of dimension $2S+1$. Taking this together with the $2S(2S+1)$ one-dimensional blocks W_{nmnm}, we obtain a matrix representation for the propagator:

$$\mathcal{U} = \mathcal{V} \otimes \mathcal{W} \qquad \mathcal{W} = \bigotimes_{n\neq m} \mathcal{W}_{nmnm} \tag{2.13}$$

whose dimension $(2S+1)^2$ is in accord with the remark above (2.5).

The frequency dependence of the self-energy is determined by the coupled density of phonon states. Since the latter function varies smoothly with frequency, we may resort to a Markov approximation, and replace the matrix elements $\Sigma(z)$ by their values at the corresponding frequencies of $\mathcal{U}(z)$.

We start with the oscillatory part of the propagator, $\mathcal{W}$, which, in terms of the density matrix (2.6), describes the time evolution of the off-diagonal operators X_{nm} with $n \neq m$. Phonon coupling leads to a loss of phase coherence, whose rate is given by

$$1/\tau_{nm} = \Im\Sigma_{nmnm}(-\Delta_{nm}) \tag{2.14}$$

The real parts $\Re\Sigma_{nmnm}$ are negligibly small. Thus we obtain

$$\mathcal{W}_{nmnm}(z) = -[z + \Delta_{nm} + \mathrm{i}/\tau_{nm}]^{-1}$$

and upon inverse Laplace transformation

$$\mathcal{W}_{nmnm}(t) = \mathrm{e}^{\mathrm{i}\Delta_{nm}t}\mathrm{e}^{-t/\tau_{nm}}. \tag{2.15}$$

Note that $\mathcal{W}$ vanishes in the long-time limit, which corresponds to the vanishing phase memory for $t \gg \tau_{nm}$.

The diagonal operators X_{nn} give rise to the zero-frequency poles with $\Delta_{nn} = 0$, i.e., the matrix Λ vanishes in the subspace spanned by X_{nn}. Accordingly we evaluate the self-energy at zero frequency,

$$R_{nm} = \Im\Sigma_{nnmm}(z=0). \tag{2.16}$$

Since $\Sigma_{nnmm}(t)$ is real and an even function of time, $\Sigma_{nnmm}(z=0)$ is purely imaginary. Thus the diagonal part of the propagator reads $\mathcal{V}(z) = -[z + \mathrm{i}R]^{-1}$, where both $\mathcal{V}(z)$ and $R \equiv (R_{nm})$ are matrices of dimension $2S+1$.

Taking the inverse Laplace transformation, we obtain the formal result

$$\mathcal{V}(t) = \mathrm{e}^{-Rt} \tag{2.17}$$

which, again, is to be read as a matrix equation, the argument of the exponential being the matrix $R = (R_{nm})$. Note that the poles of $\mathcal{V}(z)$ are purely imaginary, i.e. (2.17) does not show any oscillations. In physical terms this means that the dynamics is purely relaxational.

2.2. The rate matrix

We complete evaluation of the propagator by calculating the decoherence rates $1/\tau_{nm}$ and the relaxation rates R_{nm} as defined in (2.14) and (2.16), respectively. The double commutator in (2.9) gives rise to two types of contribution. First, there are terms which read schematically as $XVVX$ and $XXVV$ and, second, there are terms where the factors V are separated by the standard basis operators, $XVXV$. It turns out that the decoherence rates $1/\tau_{nm}$ and the diagonal entries of the rate matrix, R_{nn}, are of the first type, and the off-diagonal relaxation rates, R_{nm} with $n \neq m$, are of the second type. The latter carry a minus sign.

We start with the rate matrix R_{nm}. After inserting (1.5) in (2.9), using the spectral representation

$$\mathrm{e}^{\mathrm{i}H_S t} = \sum_n X_{nn} \mathrm{e}^{\mathrm{i}E_n t}$$

and taking advantage of (2.10), we obtain

$$\Sigma_{nnmm}(t) = \sum_k |v_{nk}|^2 \mathrm{e}^{-\mathrm{i}\Delta_{kn}t}\varphi(t)\delta_{nm} - |v_{nm}|^2 \mathrm{e}^{-\mathrm{i}\Delta_{nm}t}\varphi(t) + \mathrm{CC} \tag{2.18}$$

where the spin part of the coupling potential V reads in terms of energy eigenstates as

$$v_{nm} = \langle n|v(\boldsymbol{S})|m\rangle \tag{2.19}$$

and the bath part gives rise to the correlation function

$$\varphi(t) = \sum_s \gamma_s^2 \langle \varepsilon_s(t)\varepsilon_s(0)\rangle. \tag{2.20}$$

Its complex conjugate (CC) reads $\varphi(t)^* = \varphi(-t)$.

Upon inserting the definition of the elastic strain (1.6), assuming isotropic acoustic waves with the dispersion relation $\omega_{\boldsymbol{q}s} = v_s q$, and taking the Fourier transform, we obtain the bath spectral density

$$\varphi''(\omega) = \pi\alpha\omega^3[1 + n(\omega)]. \tag{2.21}$$

Here $n(\omega) = [\mathrm{e}^{\beta\hbar\omega} - 1]^{-1}$ denotes the Bose function and

$$\alpha = \frac{1}{2\pi^2} \sum_s \frac{\gamma_s^2}{\varrho v_s^5 \hbar} \tag{2.22}$$

a coupling constant with dimension (frequency)$^{-2}$. ϱ is the mass density. With the shorthand notation

$$\Gamma_{nm} = |v_{nm}|^2 \varphi''(\Delta_{nm}) = \pi |v_{nm}|^2 \alpha \Delta_{mn}^3 n(\Delta_{mn}) \tag{2.23}$$

one easily calculates the rate matrix R_{nm}. Its diagonal elements

$$R_{nn} = \sum_k \Gamma_{nk} \tag{2.24}$$

may be considered as the widths of the quantum levels n, whereas the off-diagonal ones

$$R_{nm} = -\Gamma_{mn} \qquad (n \neq m) \tag{2.25}$$

describe transitions between states n and m.

Now we turn to the decoherence rates $1/\tau_{nm}$. Proceeding as above and noting that $\Delta_{nm} + \Delta_{mk} = \Delta_{nk}$, we find

$$\frac{1}{\tau_{nm}} = \frac{1}{2}\sum_k \big(\Gamma_{mk} + \Gamma_{nk}\big) = \frac{1}{2}\big(R_{mm} + R_{nn}\big). \tag{2.26}$$

Equations (2.24)–(2.26) provide an explicit expression for the propagator (2.13), which we are going to apply to the relaxation of the spin variables.

It is instructive to consider the stationary solution of the propagator $\mathcal{U}(t)$. Since the off-diagonal part $\mathcal{W}$ decays exponentially, we have to look for a set of occupation numbers $p_n = \rho_{nn} = \langle X_{nn}\rangle_\rho$ fulfilling $\dot{p}_n = 0$. The equation of motion for $\rho(t) = \mathcal{V}(t)\rho(0)$ leads to the well-known Master equation

$$\dot{p}_n = \sum_m \big(\Gamma_{mn} p_m - \Gamma_{nm} p_n\big). \tag{2.27}$$

The stationary solution, or equilibrium distribution, is given by $\dot{p}_n^{(\mathrm{eq})} = 0$, which leads to the detailed-balance condition $p_n^{(\mathrm{eq})}/p_m^{(\mathrm{eq})} = \Gamma_{nm}/\Gamma_{mn} = \exp[-\beta(E_n - E_m)]$. Thus any initial state ρ will relax towards the equilibrium distribution

$$\rho^{(\mathrm{eq})} = \sum_n p_n^{(\mathrm{eq})} X_{nn}. \tag{2.28}$$

In principle, the relaxation behaviour could determined by diagonalizing the time evolution operator $\mathcal{V}$ or, equivalently, the rate matrix R, and expanding the initial state $\rho = \sum_n p_n X_{nn}$, or $\boldsymbol{p}$, in terms of the eigenvectors. In practice, such a procedure is suitable for a few system states, say not more than four. (Compare this with the treatment of the dissipative two-state system in reference [31].) Yet it is of little use for the present problem concerning $2S + 1$ spin states with, e.g., $S = 10$.

3. Magnetic relaxation

The previous sections provide the formal apparatus for the dissipative dynamics of the magnetization of a $Mn_{12}O_{12}$ molecule. Before discussing relaxation phenomena, it would seem useful to consider the time evolution of the magnetization for a given initial state.

The magnetization along the z-direction is given by the expectation value

$$M(t) = \langle S_z(t)\rangle_\rho. \tag{3.1}$$

The representation of $S_z = \sum_{nm} M_{nm} X_{nm}$ in terms of energy eigenbasis involves the coefficients $M_{nm} = \langle n|S_z|m\rangle$. When inserting the initial state (2.6) and S_z in (3.1), we find two different contributions:

$$M(t) = \sum_{n\neq m} M_{nm}\mathcal{W}^{(nm)}(t)\rho_{nm} + \sum_n M_{nn}\mathcal{V}_{nm}(t)\rho_{mm} \tag{3.2}$$

which evolve in time according to $\mathcal{W}$ and $\mathcal{V}$, respectively.

Since both ρ and M are Hermitian, the first part gives rise to terms oscillating with frequencies Δ_{nm} and whose phase coherence is lost after a time τ_{nm}. In general there are many frequencies superposed; yet with an appropriate choice for the initial state, it is in principle possible to retain a single frequency. The oscillating part vanishes for a

state which is diagonal in the energy representation, $\rho = \sum_n \rho_{nn} X_{nn}$. These oscillations of the magnetization could be probed by means of an appropriate time-dependent external field. It turns out, however, that there is little hope for observing such coherent motion; cf. section 8.4.

The second term in (3.2) is more relevant for our purpose. It describes how the magnetization tends towards its equilibrium value

$$M^{(\mathrm{eq})} = \sum_n M_{nn} \rho_{nn}^{(\mathrm{eq})}. \tag{3.3}$$

In general, this relaxation process is not uniform but occurs with rates which are given by the entries of the matrix Γ.

There are two basically different timescales. The shorter one is given by the relaxation within one well, involving transitions between states n and m with similar magnetization $M_{nn} \approx M_{mm}$. The corresponding rates are of the order of R_{nn}, i.e., they involve the largest Γ_{nm}; from (2.26) it is clear that this fast intrawell relaxation occurs on the timescale $1/\tau_{nm}$. The second characteristic time involves relaxation from one well to the other, i.e., it requires transitions between states with very different magnetization. We will see below that the corresponding transition rates Γ_{nm} are much smaller than R_{nn}.

As discussed below (3.3), the relaxation behaviour in the $(2S+1)$-dimensional spin space cannot be solved analytically. Yet the existence of two separate timescales permits us to reduce the number of variables. In view of the experimental situation, we are not interested in the occupation of each level n, but rather in the relative probability of finding the molecule in the left-hand or in the right-hand well.

The physical meaning of the double-well picture consists in positive and negative magnetization. A sound criterion for separating the $2S+1$ states in two sets is provided by considering the magnetization $M_{nn} = \langle n|S_z|n\rangle$ and by relating the probability of finding the system in the left-hand well to a negative value of M_{nn}:

$$Q = \sum_l p_l \qquad \text{for } M_{ll} < 0 \tag{3.4}$$

and similarly relating the occupancy of the right-hand well, $1-Q$, to a positive magnetization, $M_{rr} \geqslant 0$. This definition is meaningful for finite magnetic field only, since $M_{ll} = 0$ for all l in a strictly symmetric potential. Even for $B = 0$, however, the symmetry is broken by the random hyperfine field h_z; as a consequence, the case where $M_{ll} = 0$ is marginal, and Q takes in general a finite value.

When inserting the Master equation (2.27) in the time derivative of Q, we obtain

$$\dot{Q} = \Gamma_\downarrow (1-Q) - \Gamma_\uparrow Q \tag{3.5}$$

where we have defined the rates

$$\Gamma_\downarrow = \left(\sum_{lr} p_l \Gamma_{lr} \right) \Big/ \sum_l p_l = \frac{1}{Q} \sum_{lr} p_l \Gamma_{lr} \tag{3.6}$$

and $\Gamma_\uparrow$ with l and r exchanged, and Q replaced by $1-Q$. Note that, even for $Q = 1$, there is a small probability of finding the system in the right-hand well, since the energy eigenstates $|n\rangle$ are never completely localized in one well.

These rates do not depend on the occupancy Q. Because $\Gamma_{ll'} \gg \Gamma_\downarrow$, the ratio $p_l/p_{l'}$ is constant on the timescale $1/\Gamma_\downarrow$. In physical terms this means that thermal equilibrium between the states within the left-hand well is satisfied almost instantaneously, whereas the equilibration of the two wells takes a much longer time of about $1/\Gamma_\downarrow$. The rates $\Gamma_\uparrow$ and $\Gamma_\downarrow$ are weighted averages of the Γ_{nm}. As a consequence, they do not satisfy a simple detailed-balance condition, contrary to the Γ_{nm}.

In the two-well picture, magnetic relaxation is determined by the initial value $M^{(\mathrm{in})} = \langle S_z(t=0)\rangle_\rho$, the equilibrium value (3.3), and the rate $\Gamma = \Gamma_\downarrow + \Gamma_\uparrow$, according to

$$M(t) = M^{(\mathrm{eq})} + \mathrm{e}^{-\Gamma t}\big(M^{(\mathrm{in})} - M^{(\mathrm{eq})}\big). \tag{3.7}$$

In the most common experimental situation, the system is initially localized in the left-hand well, i.e. $Q = 1$. After reversing the sign of the magnetic field, however, thermal equilibrium favours the right-hand well. In (3.7) this means that $M^{(\mathrm{in})} < 0$, $M^{(\mathrm{eq})} > 0$, and $\Gamma \approx \Gamma_\downarrow \gg \Gamma_\uparrow$.

4. Energy eigenstates

The formal approach of the preceding sections strongly relied on the energy eigenstates $|n\rangle$. Since the dominant part of the energy, equation (1.1), is diagonal in terms of S_z, the angular momentum states form a most convenient basis,

$$|n\rangle = \sum_N c_N^{(n)} |N\rangle \tag{4.1}$$

with the defining equation $S_z|N\rangle = N|N\rangle$. In principle, the Hamiltonian can be written as an S-dimensional matrix that yields, upon diagonalization, the energies E_n and the corresponding eigenstates $|n\rangle$ in terms of the expansion coefficients $c_N^{(n)}$. The latter have been discussed in detail in reference [26]. Here, we will adopt a simple approximation which retains, however, all features relevant for calculating the rate $\Gamma_\downarrow$.

4.1. Pairs of resonant states

The energy scale of the diagonal part of the Hamiltonian, A, is larger than the off-diagonal one, h_x. As a consequence, the energy eigenstates differ very little from the angular momentum states, i.e., in (4.1) there is one coefficient that is close to unity, $c_M^{(m)} \approx 1$. The remaining ones are at most of the order of h_x/A, which is small, $|c_N^{(m)}| \ll 1$ for $N \neq M$. Hence the eigenstates $|m\rangle$ are well approximated by the corresponding $|M\rangle$, and the levels fulfil $E_m = E_M + Mh_z$, up to corrections of the order h_x^2/A.

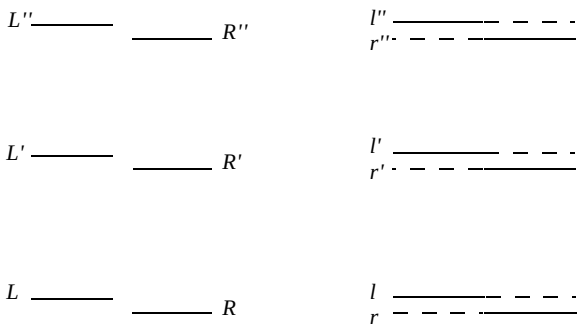

Figure 1. Angular momentum and energy eigenstates.

For certain values of the magnetic field, however, the states in the left-hand and right-hand wells, i.e., with negative and positive magnetization, form pairs of nearby levels, as shown in the left-hand part of figure 1. Then the expansion in (4.1) comprises two significant coefficients, L and R, or L' and R', etc. The remaining terms are negligible. Hence we

may truncate the Hilbert space to a resonant pair of states, with an effective Hamiltonian matrix

$$H = \begin{pmatrix} E_L + Lh_z & \frac{1}{2}\Omega_{LR} \\ \frac{1}{2}\Omega_{LR} & E_R + Rh_z \end{pmatrix} \tag{4.2}$$

where $E_N = -AN^2 - g\mu NB$. The off-diagonal terms are calculated perturbatively in powers of h_x/A; we quote the result

$$\Omega_{NM} = \frac{2A}{(N-M-1)!^2}\sqrt{\frac{(S+N)!(S-M)!}{(S-N)!(S+M)!}}\left(\frac{h_x}{2A}\right)^{N-M} \tag{4.3}$$

for $N > M$ [7, 21].

After subtracting the average energy and defining the asymmetry energy

$$\epsilon_{LR} = E_L - E_R + (L-R)h_z \tag{4.4}$$

one easily calculates the eigenvalues of (4.2)

$$E_\pm = \frac{1}{2}[E_L + E_R + (L+R)h_z] \pm \frac{1}{2}\sqrt{\Omega_{LR}^2 + \epsilon_{LR}^2} \tag{4.5}$$

and the corresponding eigenvectors

$$|+\rangle = u|L\rangle + \sqrt{1-u^2}|R\rangle \tag{4.6}$$

$$|-\rangle = \sqrt{1-u^2}|L\rangle - u|R\rangle \tag{4.7}$$

where we have dropped the labels LR and defined the quantity

$$u^2 = \frac{1}{2}\left(1 - \frac{\epsilon}{\sqrt{\Omega^2+\epsilon^2}}\right). \tag{4.8}$$

Corrections to the approximate energies $E_\pm$ and eigenstates $|\pm\rangle$ are of the order of (h_x/A).

The coefficient u has been chosen such that, for positive ϵ_{LR}, the state of the upper level $|+\rangle$ has a larger amplitude in the right-hand well, and the lower in the left-hand well; we will use the suggestive notation

$$|l\rangle = |\mp\rangle \qquad |r\rangle = |\pm\rangle \qquad \text{for } \epsilon_{LR} \gtrless 0. \tag{4.9}$$

(For the marginal case of zero bias, $\epsilon_{LR} = 0$, the two states have equal amplitudes in the two wells, $|\pm\rangle = 2^{-1/2}(|L\rangle \pm |R\rangle)$.) Equation (4.9) ensures that the angular momentum states $|L\rangle$ (or $|R\rangle$) provide the largest amplitude to the energy eigenstates $|l\rangle$ (or $|r\rangle$).

The right-hand part of figure 1 illustrates the hybridization of resonant levels. The states $l, r, l', r', \ldots$ are no longer localized in one well or the other; yet we have indicated the smaller amplitude by a broken line on the left- or right-hand side. According to (4.9), we have plotted the levels for positive ϵ_{LR}. A negative value would result in an exchange of the labels l and r, etc, and of solid and broken lines.

The superposition of resonant states is essential for two physical effects. First, it lies at the origin of level repulsion; when switching the magnetic field through a resonance, no real degeneracy occurs, since the off-diagonal energies Ω_{NM} provide a minimum splitting. Second, the amplitudes u and $\sqrt{1-u^2}$ describe the mixing of states from different wells, and thus give rise to relaxation from one well to the other.

5. The transition rates Γ_{nm}

According to (3.6) the magnetic relaxation behaviour is determined by the off-diagonal entries of the rate matrix, Γ_{nm}. In view of (2.23), we need to calculate the energy difference Δ_{nm} and the coupling matrix element v_{nm} as defined in (2.19). In the following, we discuss the rates for transitions between energy eigenstates in the two wells.

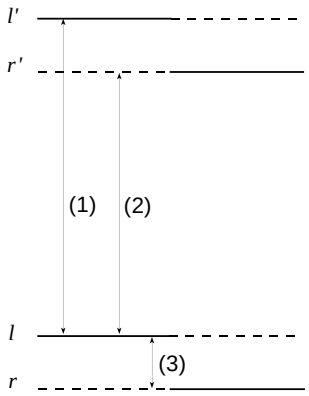

Figure 2. Phonon-assisted transitions between energy eigenstates. For details see the main text.

5.1. Intrawell relaxation (1)

First we consider transitions between states $|l\rangle$ and $|l'\rangle$ that have a larger amplitude in the left-hand well; cf. (1) in figure 2. These rates do *not* contribute to the relaxation into the right-hand well, but govern how thermal equilibrium is reached within the left-hand well.

According to the above discussion, we have

$$|l\rangle = \sqrt{1-u^2}|L\rangle + u|R\rangle$$

and a similar expression for $|l'\rangle$, with amplitudes u and u' given by (4.8) for the pairs L, R and $L+1, R-1$. With the matrix element of (1.7) connecting angular momentum eigenstates,

$$\langle N+1|v|N\rangle = (N+\tfrac{1}{2})\sqrt{S(S+1)-N(N+1)} \equiv c_N \tag{5.1}$$

one easily finds

$$v_{ll'} = c_L\sqrt{(1-u^2)(1-u'^2)} + c_R u u'. \tag{5.2}$$

For positive asymmetry energy ϵ, one quickly reaches the range $u, u' \ll 1$ where the second term is of little significance. Except for marginal cases, the approximate expression

$$v_{ll'} \approx (L+\tfrac{1}{2})\sqrt{S(S+1)-L(L+1)}. \tag{5.3}$$

correctly describes the rate. Since the hybridization energy is much smaller than the diagonal terms, the energy difference $\Delta_{ll'}$ is well approximated by

$$\hbar\Delta_{l'l} \approx -A(2L'+1) - g\mu B. \tag{5.4}$$

As is clear from (2.24) and (2.26), the intrawell relaxation rates determine the level width R_{nn} and the characteristic time for the loss of phase memory of the tunnel oscillations, τ_{nm}. With the parameters discussed below, one finds typical values of 10^9–10^{11} s^{-1}.

5.2. Non-diagonal resonances (2)

Now we turn to transitions from states mainly localized in the left-hand well, l, l', l'', ..., to those in the right-hand well, r, r', r'', ...; cf. (2) in figure 2. A particularly interesting situation arises for a magnetic field close to the resonant values defined in (1.2).

Naively, one would expect transitions through resonant level pairs $l \leftrightarrow r$, $l' \leftrightarrow r'$, etc, to be the most significant. It turns out, however, that this is not the case; the magnetic relaxation behaviour is governed by transitions like $l \leftrightarrow r'$ and $l' \leftrightarrow r$, i.e. between states that belong to adjacent resonant pairs (cf. figure 1).

We first consider the rate $\Gamma_{lr'}$, which depends on the energy difference $\Delta_{lr'}$ and the matrix element of the operator (1.7), $v_{lr'} = \langle l|v(\boldsymbol{S})|r'\rangle$. The former differs little from the energy difference of the corresponding angular momentum eigenstates

$$\Delta_{lr'} \approx (E_L - E_{R'} + Lh_z - R'h_z)/\hbar \tag{5.5}$$

whereas the matrix element $v_{lr'}$ reads with (4.8) and (5.1) as

$$v_{lr'} = c_L u\sqrt{1-u'^2} - c_{R-1}\sqrt{1-u^2}u'. \tag{5.6}$$

With $\Delta_{r'l} = -\Delta_{lr'}$ we find the transition rate

$$\Gamma_{lr'} = \pi v_{lr'}^2 \alpha \Delta_{r'l}^3 n(\Delta_{r'l}). \tag{5.7}$$

At resonance, $\epsilon = 0 = \epsilon'$, we have $v_{lr'} = \frac{1}{2}(c_L - c_{R-1})$. In real systems, however, this case is marginal, because of the random hyperfine interaction h_z. (See section 6 below.) As a consequence, the matrix element $v_{lr'}$ is in general much smaller than unity, contrary to the case for intrawell transitions, where $v_{ll'}$ is of the order of $S^{3/2}$, for not too small $|l|$.

The rate (5.7) is smaller by an overlap factor $u^2(1-u'^2)$ than that for intrawell relaxation. This is why the interwell relaxation is so much slower than the motion within one well.

5.3. Direct resonant transitions (3)

Finally we consider phonon-assisted transitions within a resonant level pair, $l \leftrightarrow r$, labelled (3) in figure 2. Although formally identical to (5.7), the corresponding rate is much smaller, since both the matrix element v_{lr} and the energy difference

$$\hbar\Delta_{lr} = \sqrt{\Omega_{LR}^2 + \epsilon_{LR}^2}$$

are significantly reduced.

At very low temperatures and small magnetic field, however, the non-diagonal resonances become ineffective, because of the exponentially small factors $n(\Delta_{r'l})$. Then the resonant rate between the ground states in the two wells, $l = -10$ and $r = 10$, dominates the magnetic relaxation behaviour. (We recall that l, r denote energy eigenstates, where l has a larger amplitude in the left-hand well, and r in the right-hand one.)

Therefore we evaluate (4.2)–(4.9) for the special case where $R = -S$, $L = S$, and small but finite magnetic field, $g\mu B \ll A$. With $\Omega = \Omega_{-S,S}$ and $\epsilon \equiv E_{-S} - E_S - 2Sh_z$, where $E_{-S} - E_S = g\mu 2SB$, the two-state Hamiltonian reads as

$$H = \frac{1}{2}\begin{pmatrix} \epsilon & \Omega \\ \Omega & -\epsilon \end{pmatrix}. \tag{5.8}$$

With the matrix element $v = \langle l|v(\boldsymbol{S})|r\rangle$ and the energy splitting of the ground states $\hbar\Delta = \sqrt{\Omega^2 + \epsilon^2}$, we obtain the rate for direct transitions

$$\Gamma_{\rm dir} = \pi v^2 \alpha \Delta^3 [n(\Delta) + 1]. \tag{5.9}$$

Now we are going to evaluate the phonon scattering matrix element connecting the ground-state doublet, v. Unlike in the cases considered above, it is not sufficient to retain the amplitudes of two angular momentum states, $N = \pm 10$; in order to obtain a finite v, we have to take into account the amplitudes of the adjacent states $N = \pm 9$ as well.

The amplitudes of the lowest angular momentum states $|S\rangle$ and $|-S\rangle$ are determined by the two-state Hamiltonian, and read u and $\sqrt{1-u^2}$. Since the transverse field $S_x h_x$ is smaller than the energy difference of adjacent angular momentum states, the coefficients for $N = \pm 9$ can be calculated perturbatively in terms of $S_x h_x$ or, more precisely, in terms of the small parameter $x = \langle N = 10|S_x h_x|N = 9\rangle/(E_9 - E_{10})$. Starting from the largest amplitudes u and $\sqrt{1-u^2}$, we find

$$\begin{aligned} c_{-10}^{(l)} &= \sqrt{1-u^2} = c_{10}^{(r)} \qquad & c_{10}^{(l)} &= u = -c_{-10}^{(r)} \\ c_{-9}^{(l)} &= x\sqrt{1-u^2} = c_{9}^{(r)} \qquad & c_{9}^{(l)} &= xu = -c_{-9}^{(r)}. \end{aligned} \tag{5.10}$$

The remaining amplitudes with $-8 \leqslant N \leqslant 8$ are of the order of x^2 and hence may be neglected. The coefficients (5.10) are normalized up to corrections of the order x^2.

Now it straightforward to calculate the matrix element $v = \langle l|v(\boldsymbol{S})|r\rangle$. Inserting the small parameter

$$x = \frac{\sqrt{S/2}b_x}{(2S-1)A} \tag{5.11}$$

the matrix element $\langle N = 10|\{S_z, S_x\}|N = 9\rangle = (S - \frac{1}{2})\sqrt{2S}$, and the square of the overlap

$$u^2(1-u^2) = \frac{1}{4}\frac{\Omega^2}{\Omega^2 + \epsilon^2} \tag{5.12}$$

we obtain an explicit result:

$$v^2 = (S - 1/2)^2 2Sx^2u^2(1-u^2). \tag{5.13}$$

Inserting this in (5.9) and dropping terms of the order $1/S$, we find the rate for direct transitions between the states of the ground-state doublet:

$$\Gamma_{\rm dir} = \pi(Sb_x/A)^2\alpha(\Omega/\hbar)^2\Delta[n(\Delta)+1]. \tag{5.14}$$

Anticipating a more detailed discussion to be given below, we remark that $\Gamma_{\rm dir}$ is independent of the magnetic field and proportional to T for $2Sg\mu|B| < k_{\rm B}T$, whereas it varies *linearly* with B and is constant with respect to T at very low temperatures $k_{\rm B}T < 2Sg\mu|B|$.

We briefly discuss two discrepancies between the rate (5.14) and previous results [17, 24, 26], concerning the dependence on the magnetic field B.

(i) In these studies, a quadratic law, $\Gamma \propto B^2$, is derived for the most relevant case, that where $2Sg\mu B < k_{\rm B}T$, and a cubic law, $\Gamma \propto B^3$, for $k_{\rm B}T < 2Sg\mu B$. This result is obtained from an expression that, for finite magnetic field, is identical to our equation (5.9), with $\hbar\Delta \approx 2Sg\mu B \gg \Omega$. As is obvious from (5.12), however, the overlap matrix element connecting the left-hand and right-hand states provides, for $\epsilon \equiv 2Sg\mu B \gg \Omega$, a factor Ω^2/ϵ^2; this additional factor reduces the power of B by 2, and leads to a rate independent of B for $\epsilon < k_{\rm B}T$, and a linear variation in the opposite case.

(ii) The rate of reference [17] vanishes in the limit of zero field, whereas our expression tends towards

$$\Gamma_{\rm dir} = \pi(Sb_x/A)^2\alpha(\Omega/\hbar)^3[n(\Omega/\hbar)+1] \qquad (B=0). \tag{5.15}$$

In [17], this constant term is missed since the perturbation expansion is carried out in terms of angular momentum eigenstates $|N\rangle$. Hence the energy splitting of resonant states does not account for level repulsion due to the finite off-diagonal energy Ω. Accordingly, at zero magnetic field the phonon spectral density is evaluated at zero frequency, resulting in a vanishing rate, whereas our rate remains finite at $B = 0$.

In summary, our results differ from that obtained in [17, 24, 26], since in these studies the magnetic field dependence of the factor v^2 has been neglected. Moreover, our perturbation expansion is based on energy eigenstates, rather than the angular momentum basis used in [17].

6. The average over the hyperfine field

The fields h_x and h_z introduced in (1.3) account for the hyperfine interaction of the nuclear spin, with $I = \frac{5}{2}$ for ^{55}Mn, with the electronic spin, $\sigma = 2$ for Mn^{3+} and $\sigma = \frac{3}{2}$ for Mn^{4+}. Whereas for a single Mn atom, this coupling is simply given by $A_{\rm hf}\boldsymbol{\sigma} \cdot \boldsymbol{I}$, a more complicated situation is encountered in the case of the $Mn_{12}O_{12}$ molecule. The strong magnetic interaction favours collective spin states with $S = 10$ that are only weakly perturbed by the nuclear spins.

Hartmann-Boutron *et al* [26] have studied in detail the level splitting and degeneracies resulting from the hyperfine interaction. They find that coupling to nuclear spins gives rise to a few hundred levels spread over an energy range of about 1 K; the hyperfine field takes values of the order 0.1 T.

Here, we neglect the microscopic structure of this coupling. Instead, we use the simple form (1.3) with random fields h_x and h_z. The hyperfine interaction has two physical effects. Its off-diagonal part $h_x S_x$ mixes the angular momentum states, whereas the diagonal term $h_z S_z$ acts as an additional magnetic field along the magnetization axis.

The values of the fields h_x and h_z depend on the nuclear spin state of the 12 Mn atoms which varies from one molecule to another and as a function of time. In order to account for the resulting randomness, we introduce a distribution law for the hyperfine fields. The actual discrete spectrum is well approximated by a Gaussian [26]:

$$P_i(h_i) = \frac{1}{\sqrt{2\pi}\, b_i} \exp\left(-\frac{h_i^2}{2b_i^2}\right) \tag{6.1}$$

where $b_i/k_{\rm B}$ is of the order of 0.1 K.

The average over h_x concerns the off-diagonal energies Ω_{NM}, as defined in (4.3). We will assume that the Ω_{NM} involve already the properly averaged fields, i.e., we replace h_x by b_x.

We are rather interested in the dependence on h_z of the phonon scattering matrix elements v_{lr}. The field h_z adds a random component to the static magnetic field B. According to (4.4), this results in a distribution for the asymmetry energy ϵ_{LR} between the resonant states $|L\rangle$ and $|R\rangle$. On the other hand, this random field is irrelevant for non-resonant levels, since b_z is significantly smaller than a typical level spacing $\hbar\Delta_{ll'}$.

As a result, the average over h_z concerns the matrix elements $v_{lr'}^2$ for the non-diagonal resonances, equation (5.7), whereas in the direct transitions, equation (5.14), it merely affects the level spacing Δ_{lr}. The intrawell relaxation is hardly modified by the hyperfine field.

6.1. Non-diagonal resonances

The average over h_z in $v_{lr'}^2$ concerns the asymmetry energies ϵ and ϵ' in the amplitudes u and u' of equation (5.6). The ensuing integral

$$\int {\rm d}h \;\; P(h) v^2$$

could be calculated numerically; yet a slight simplification of the field dependence will permit us to obtain an analytic result.

We start with a few remarks concerning (5.6). (i) Except for very large magnetic fields, we have $c_L \approx -c_{R-1}$. (ii) For states not too close to the top of the barrier, we have $\Omega_{LR} \ll b_z$, resulting in $u \ll u' \ll 1$ for $\epsilon > 0$ and $(1-u^2)^{1/2} \ll (1-u'^2)^{1/2} \ll 1$ for $\epsilon < 0$. As a consequence, we may replace u by $\Theta(-\epsilon)$ and $(1-u^2)^{1/2}$ by $\Theta(\epsilon)$. With (i) and (ii), the average $\overline{v^2}$ reads as

$$\overline{v_{lr'}^2} = \frac{1}{4}(c_L - c_{R-1})^2 \left\{ \overline{u'^2 \Theta(\epsilon')} + \overline{(1-u'^2)\Theta(-\epsilon')} \right\} \tag{6.2}$$

with

$$\overline{f(h)} = \int \mathrm{d}h \; P(h) f(h).$$

From (4.8) it is clear that the expression in brackets is sharply peaked about

$$\epsilon = E_{L'} - E_{R'} + (L' - R')h \approx 0.$$

Since the weight $P(h)$ is a much smoother function, it may be evaluated at

$$h = -(E_{L'} - E_{R'})/(L' - R').$$

The remaining integral is equal to Ω', resulting in

$$\overline{v_{lr'}^2} = \frac{1}{4}(c_L - c_{R-1})^2 P\left(\frac{E_{L'} - E_{R'}}{L' - R'} \right) \Omega'. \tag{6.3}$$

Note the correspondence $l \leftrightarrow L$, $l' \leftrightarrow L'$, etc. Primed quantities such as Ω' refer to resonant angular momentum states L' and R'; cf. figure 1. The asymmetry ϵ is the same for all such pairs.

The averaged matrix element $\overline{v^2}$ shows two remarkable features, as a function of ϵ and Ω'. For small asymmetry, i.e., close to resonance, the quantity $P\Omega'$ takes its maximum value. As soon as $|E_{L'} - E_{R'}|$ exceeds the hyperfine field, $\overline{v^2}$ falls off quickly.

The energy distance for transitions through non-diagonal resonances, $\Delta_{lr'}$, is of the order of SA, which is much larger than the hyperfine field b_z. Hence the average of the rate (5.7) reads as

$$\overline{\Gamma_{lr'}} = \pi \overline{v_{lr'}^2} \alpha \Delta_{r'l}^3 n(\Delta_{r'l}). \tag{6.4}$$

The main effect of the hyperfine coupling h_z consists in a broadening of the resonance as a function of the bias $\epsilon \propto B - B_J$. For $h_z = 0$, the factor $v_{lr'}^2$ would give rise to a sharp peak of width Ω' at $\epsilon = 0$, i.e. at the resonance values of the magnetic field B. The presence of h_z leads to a distribution of such resonances with width b_z. As a consequence, the rate $\Gamma_{lr'}$ shows a broad bump as a function of B about the values B_J defined in (1.2); the maximum value is reduced by a factor $P(0)\Omega' = (\Omega'/\pi b_z)$.

6.2. Direct transitions

Finally we consider how relaxation through the direct process between the ground-state doublet is affected by the hyperfine field. The rate (5.14) depends on h_z through the energy $\hbar\Delta = \sqrt{\Omega^2 + \epsilon^2}$ in the factor $\Delta[1 + n(\Delta)]$. At finite temperature the rate

$$\overline{\Gamma_{\mathrm{dir}}} = \pi (S b_x / A)^2 \alpha (\Omega/\hbar)^2 k_{\mathrm{B}} T/\hbar \qquad (\hbar\Delta \ll k_{\mathrm{B}} T) \tag{6.5}$$

depends on the off-diagonal element Ω and T only.

In the limit of zero temperature, the nuclear spins are frozen in the ground state with respect to the hyperfine coupling, and h_z is no longer a random variable but takes a fixed value. The resulting rate reads as

$$\overline{\Gamma_{\mathrm{dir}}} = \pi (S b_x / A)^2 \alpha (\Omega/\hbar)^2 \Delta \qquad (T = 0) \tag{6.6}$$

with $\hbar\Delta = \sqrt{\Omega^2 + (g\mu SB)^2}$, where the magnetic field B may include a small contribution from the hyperfine coupling.

7. Discussion

Here we discuss our formal result (3.6) as regards its dependence on temperature and magnetic field. We focus on the range of parameters that are covered by available experiments. For a discussion of the parameters, see section 7.4 below.

According to (3.6), magnetic relaxation is governed by a weighted average of the rates Γ_{lr}. When starting from an initial state where only states localized in the left-hand well are populated, we have $Q = 1$. For times that are not too long, the rate is given by

$$\Gamma_{\downarrow} = \sum_{lr} p_l \overline{\Gamma_{lr}} \tag{7.1}$$

where the bar denotes the average over the hyperfine field h_z. More explicitly, these initial conditions mean that $p_r = 0$ for all r in the right-hand well, whereas the states in the left-hand well are occupied according to $p_{l=-S} \approx 1$ and $p_l \ll 1$ for $l > -S$.

As discussed in the preceding section, both direct transitions $l = -r$ and non-diagonal resonances $l = -r \pm 1$ may contribute significantly to the double sum in (7.1). Except for very low temperatures and small magnetic field, however, the direct ones are irrelevant.

7.1. Magnetic field dependence

Figure 3 shows $\Gamma_{\downarrow}$ as a function of B, for several temperatures varying from 2 to 3 K. As discussed above, the rate is strongly enhanced at the values (1.2) of the magnetic field. According to (6.3) and (6.4), the shape of these resonances is determined by the distribution of the hyperfine field, $P_z(h_z)$, and their width is given by b_z.

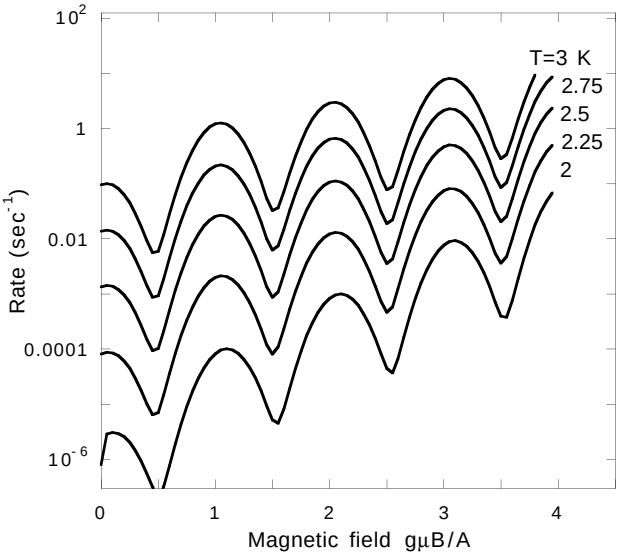

Figure 3. The magnetic relaxation rate (7.1) as a function of the external field B for several temperatures. The parameters used are discussed in section 7.4.

Besides the strong enhancement at $B = B_J$, the rate shows an overall increase as a function of the magnetic field, since the number of intermediate states decreases in the perturbation series for Ω_{LR}, thus enhancing the off-diagonal matrix element Ω_{LR}.

The curves plotted in figure 3 account for data observed by several groups [12–15]. The dependence on B and T agrees qualitatively with that reported in [13], although the variation with T is somewhat stronger than is shown by the data, and the resonance shape is not quite the same. A possible enhancement of the rate at the even resonances $J = 0, 2, \ldots$ due to a transverse crystal field is discussed below.

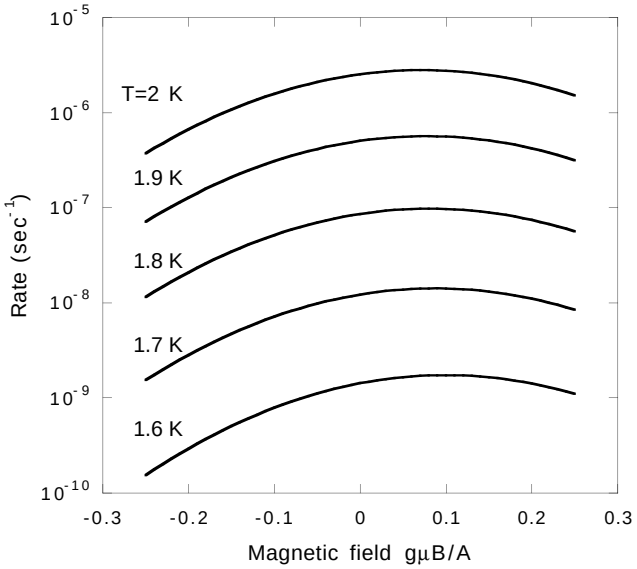

Figure 4. The magnetic relaxation rate (7.1) as a function of the external field close to $B = 0$ for several temperatures. The parameters are discussed in section 7.4.

When considering the field dependence more closely, one finds that the maxima do not occur at $B = B_J$, but are shifted to slightly higher values of the magnetic field. This asymmetry is shown in figure 4 for the resonance about $B = 0$ at several temperatures. The physical mechanism for this effect is most easily understood in terms of figure 2, with the initial state $l = -S$. The most efficient relaxation channel involves the excited resonance labelled (2). For small but positive magnetic field, the activation energy is reduced by $2Sg\mu B$, and the rate increases accordingly; as soon as the field exceeds the longitudinal hyperfine coupling h_z, the overlap matrix element $\overline{v^2}$ is strongly suppressed. Thus the maximum occurs at $B \approx b_z$.

Barbara *et al* [16] have studied the asymmetry of the resonance at $B = 0$ in detail, and found a behaviour similar to that of figure 4, though the observed maxima are more pronounced than those in our figure. (Compare this with the remark in section 7.4.)

In the limit of zero temperature and finite but not too large magnetic field, $\Omega < 2g\mu SB \ll A$, the relaxation is governed by the direct rate $\Gamma_{\rm dir}$. In this range, we expect a *linear* variation of the rate with the magnetic field:

$$\Gamma_{\rm dir} \propto \Omega^2 B \qquad (T = 0) \tag{7.2}$$

according to (6.6). This linear law arises from the product of two factors in $\Gamma_{\rm dir}$. Evaluating the cubic bath spectral density (2.21) at the ground-state splitting $\Delta \approx 2Sg\mu B/\hbar$ gives rise

to B^3, as derived in [17]; there are, however, the overlap matrix elements $u^2(1-u^2)$ in v^2 that give, for $\epsilon = 2Sg\mu B > \Omega$, a factor $\Omega^2/(2Sg\mu B)^2$, according to (5.12).

Equation (7.2) is valid for $k_BT < 2Sg\mu B$; in the opposite case the magnetic field has to be replaced by temperature:

$$\Gamma_{\rm dir} \propto \Omega^2 T \qquad (2Sg\mu B < k_BT \ll A) \tag{7.3}$$

resulting in a rate that is independent of the magnetic field. Note that $\Gamma_{\rm dir}$ is significantly smaller than the rate derived in [17, 26].

7.2. Temperature dependence

Each contribution to the relaxation rate $\Gamma_\downarrow$ consists of two factors that both depend on temperature. *First*, the occupation number $p_l \propto \exp(-E_l/k_BT)$ varies exponentially with the energy distance from the ground state in the left-hand well. The higher the energy of the excited state E_l, the smaller the corresponding Boltzmann factor. *Second*, the variation of the transition rate Γ_{lr} with l and r arises mainly from the factor Ω in the averaged overlap matrix elements $\overline{v_{lr}^2} \propto P\Omega$. The Bose factor that accounts for the different weights of phonon emission and absorption gives rise to a temperature dependence.

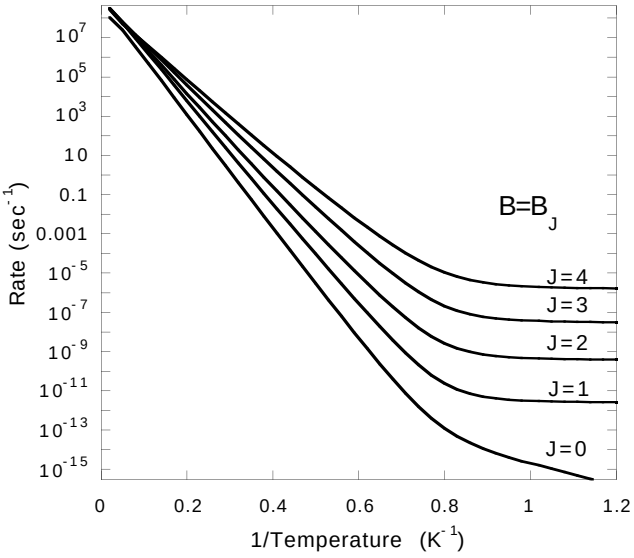

Figure 5. The magnetic relaxation rate (7.2) as a function of inverse temperature. The parameters are discussed in section 7.4.

For $B \geqslant 0$, the rate (7.1) may obey various laws as a function of temperature. At low T, the behaviour for a magnetic field above the first resonant value, $g\mu B \geqslant A$, is very different from that at smaller field. For this reason, we discuss the two cases separately. Numerical results obtained from equation (7.1) for several values of B are plotted in figure 5.

7.2.1. Small magnetic field. We start with the case where $B \ll A/g\mu$. In the limit of very low temperature, the Boltzmann factors p_l of all excited levels vanish, and the rate is determined by transitions between the ground states in the two wells, $l = -S$ and $r = S$, that are almost degenerate, $\hbar\Delta_{-S,S} \ll A$; as a consequence, the factor arising from the

phonon spectral density is very small. The resulting rate $\Gamma_{\rm dir}$ is constant at $T = 0$, and varies linearly with temperature at finite T, as discussed above. Relaxation occurs on a very long timescale that may well not be accessible experimentally. This range is *not* visible in figure 5, since the rate $\Gamma_{\rm dir}$ is out of the range shown by orders of magnitude.

As temperature increases, non-diagonal resonances, such as from $l = -S$ to $r = S - 1$, or $l = -S + 1$ to $r = S$, become more efficient. The resulting rate obeys an Arrhenius law with activation energy $V = E_{-S+1} - E_{-S} = (2S - 1)A$. The curve for $B = 0$ in figure 5 shows precisely this behaviour in the range below 1.5 K.

On further increasing the temperature, however, transitions between resonant level pairs not far from the top of the barrier prevail, because of the much larger overlap $\overline{v^2}$. As a consequence, the relaxation rate $\Gamma_\downarrow$ shows activated behaviour with an energy V that is of the order of the barrier height S^2A.

Arrhenius behaviour with two different activation energies at $B = 0$ has been observed by Barbara *et al* [16]. There is a slight discrepancy concerning the crossover temperature; the change in the activation occurs at 2 K, whereas from figure 5 one finds rather 1.4 K. (Compare this with the remark in section 7.4.)

7.2.2. Finite magnetic field, $g\mu B \geqslant A$. At low temperature, the behaviour is very different from that observed at small field. The relevant transitions occur from $l = -S$ to $r = S, S - 1, S - 2, \ldots$ for $B \approx B_J$, with $J = 1, 2, 3, \ldots$. Accordingly, the phonon spectral density φ'' has to be evaluated at energies Δ_{lr} that are of the order SA, and the resulting rates are larger than in the case where $B \approx 0$ by many orders of magnitude.

For temperatures well below the first excited level, $k_{\rm B}T \ll SA$, the rate is constant; this behaviour is shown in figure 5 below 1.5 K. With (5.7), $l = -S$, $r = S - J$, and $B \approx JA/g\mu$, the relevant contribution to $\Gamma_\downarrow$ reads as

$$\Gamma_{-S,S-J+1} = \pi v^2_{-S,S-J+1} \alpha \Delta^3_{r'l}. \tag{7.4}$$

Hence the dominant transitions do *not* occur between degenerate levels $-S$ and $S - J$, but from $-S$ to that *below* $S - J$. Going from J to $J + 1$ enhances the rate by about two orders of magnitude, since the overlap matrix element $v_{-S,S-J+1}$ strongly increases with decreasing $|l - r| = 2S - J$.

Above 1.5 K, relaxation from excited levels $l > -S$ becomes relevant. Since transitions close to the top of the barrier are most efficient, the rate shows Arrhenius behaviour:

$$\Gamma_\downarrow = \Gamma_0 \exp(-V/k_{\rm B}T) \tag{7.5}$$

where the activation energy is given by the energy of the lowest level in the left-hand well, $V = E_{-S}$.

The absolute value of $E_{-S} = -S^2A + Sg\mu B$ decreases with rising B; therefore a finite magnetic field lowers the effective activation energy. This effect is clearly seen in figure 5, where the temperature dependence of the rate above 2 K is well described by

$$V = S^2A - Sg\mu B. \tag{7.6}$$

Activated behaviour of the rate has been reported by several authors [9, 10, 12–16] for $Mn_{12}Ac$ in the temperature range from 2 to 10 K. The activation energy of $V = 61$ K at $B = 0$ agrees with (7.5). There is some evidence that increasing the magnetic field reduces V [10], in accordance with (7.6).

As discussed by Villain *et al* [19], the prefactor of (7.5) is given by the rates Γ_{lr} close to the top of the barrier. There is no rigorous way of mapping the exact expression (7.1)

onto the simpler law (7.5). Yet it is clear that Γ_0 is approximately given by the transitions from $l = 0$ to $r = 1$ [19]. Inserting $v_{01}^2 \approx S^2(\Omega_{01}^2/\Delta_{01}^2)$, the corresponding overlap energy

$$\Omega_{01} = b_x\sqrt{S(S+1)}$$

and level splitting $\hbar\Delta_{01} \approx A$, we find

$$\Gamma_0 \approx \pi\alpha S^2\Omega_{01}^2 A\hbar^{-3} = \pi\alpha S^3 b_x^2 A/\hbar^3. \tag{7.7}$$

At first sight, the Arrhenius law shown in figure 5 is somewhat surprising since each contribution to (7.1) involves a level spacing Δ_{lr} that is at most of the order SA. As pointed out above, the matrix elements $\overline{v^2}$ strongly favour transitions close to the top of the barrier; the temperature dependence of the corresponding population factor p_l gives rise to the activation energy V.

7.3. Quartic corrections to the crystal field

Regarding the crystal field in the energy (1.1), we have retained the quadratic term along the easy axis S_z only. Here we briefly discuss the relevance of higher-order components, both parallel and perpendicular to the z-axis. For symmetry reasons, these terms are of at least fourth order in the spin operators S_i.

The energy levels of a $Mn_{12}Ac$ molecule are well described by the crystal-field and Zeeman terms (1.1), which are diagonal in the spin component S_z. Yet there is some experimental evidence that the quartic correction

$$-A_4S_z^4 \tag{7.8}$$

is not really negligible as compared to the quadratic term $-AS_z^2$. From EPR data [9], Hartmann-Boutron *et al* derived $A_4/A \approx 0.006$ [26]. With such a finite quartic term, the resonances of angular momentum states $|-M\rangle$ and $|M-J\rangle$ do no longer occur at B_J as given in (1.2), but at several values $B_J(M)$ spread about B_J.

In figure 6 we plot the rate arising from (1.4) supplemented with a quartic contribution $-A_4S^4$, where $A_4/A = 0.002$. There are two sets of resonances; at $T = 1.4$ K the rate is maximum at values for B of about $1.4A/g\mu$ and $2.7A/g\mu$. With increasing temperature, the maxima are shifted towards $B = B_J$. Such a behaviour has been reported by Barbara *et al* [16]. Though smaller by a factor of 3, our value for A_4/A is of the same order as that derived from EPR data [9, 26].

The transverse terms, i.e., those involving S_x^4 and S_y^4, give rise to an off-diagonal part of the Hamiltonian that reads, in terms of angular momentum states,

$$-C(S_+^4 + S_-^4). \tag{7.9}$$

Unlike the hyperfine interaction (1.3), the transverse crystal field (7.9) mixes only angular momentum states with $\Delta M = \pm 4$. Hartmann-Boutron *et al* [26] have studied in detail the energy eigenstates and the relaxation dynamics arising from a phonon coupling potential (1.5) with various choices for the operator $v(\boldsymbol{S})$.

When using (7.9) instead of the transverse hyperfine coupling S_xh_x, we would find a very different behaviour for odd resonances $J = 1, 3, 5, \ldots$ and even ones $J = 2, 4, \ldots$ in (1.2). In fact, the relaxation rate would be large at the even ones, whereas the odd resonances would be blocked.

Since such an effect is hardly visible in the data reported in references [13, 14], we conclude that the transverse part of the Hamiltonian is dominated by the hyperfine coupling. On the other hand, the data of reference [15] show, at 2.1 K, a rate that is larger at $J = 0$ than at $J = 1$; yet this discrepancy arises at 2.1 K only—for higher temperatures the value

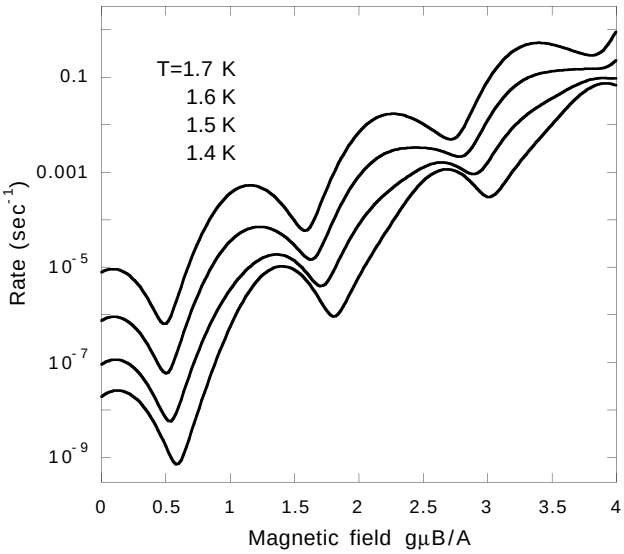

Figure 6. The relaxation rate as a function of B; as in figure 3, but with the finite quartic term (7.8). For the phonon coupling, we have used $\alpha = 1.25 \times 10^{-33}$ s^2.

at the resonances increases with J. Again, this would indicate that there is a small but finite transverse crystal field. In a very recent paper, Luis *et al* have investigated the interplay of such a quartic transverse crystal field and hyperfine or dipolar interactions [22].

7.4. Parameters

Finally we discuss the parameters used for our plots. The parameter of the crystal field A takes a value of about 0.6 K [9]; our values for the hyperfine fields $b_x = 0.45A$ and $b_z = 0.15A$ are close to that obtained by Hartmann-Boutron *et al* [26], $b = 0.15A$. The better agreement with experimental data is the reason for our choosing b_x three times larger than b_z.

We suspect that the simple form of the longitudinal hyperfine coupling is responsible for this discrepancy. The actual interaction with nuclear spins may well be more complicated than (1.3); cf. appendix E of [26].

The phonon coupling constant (2.22) provides an overall factor for the rate; its dimension is (time)^2. With the exception of in figure 6, we have put $\alpha = 1.25 \times 10^{-37}$ s^2, corresponding to an elastic deformation potential γ / k_B of about 0.1 K. When taking account of the factor $S^{3/2}$ carried by the matrix element (1.7), we find a value between 1 and 10 K, which is identical to the deformation potential given by Abragam and Bleaney for spin–lattice coupling of rare-earth ions (cf. section 10.4. of reference [32]).

We should note that the agreement with a given data set could be significantly improved by varying the parameters. It is worthwhile to mention that the crossover temperature of figure 5 could be adjusted to the observed value of 2 K with a larger value of b_x. On the other hand, this would lead to much too large a prefactor Γ_0. Again, both features could be improved by introducing additional parameters, e.g., a finite transverse crystal field (7.9).

8. Miscellaneous comments

8.1. Perturbation theory

Our perturbation theory of the reduced propagator constitutes a controlled approximation in terms of the spin–phonon coupling. It is essential that the perturbation expansion is performed in the *energy eigenbasis* of the spin system, rather than in the angular momentum states. As a second approximation, we have expanded the coefficients of the energy eigenstates in terms of the small energies Ω_{NM} and retained the leading contributions only.

To second order in the phonon coupling, the dynamics of the off-diagonal basis operators X_{nm}, with $n \neq m$, is such that they decouple from the diagonal ones, X_{nn}. As a consequence, the Liouville matrix factorizes into two corresponding blocks $\mathcal{V}$ and $\mathcal{W}$. We emphasize that this decoupling occurs only in a Liouville basis X_{nm} composed of energy eigenstates $|n\rangle$ of the spin part of the Hamiltonian.

The choice of the energy eigenbasis permits us to avoid a problem that is encountered when using the angular momentum eigenbasis. To see this, we note that the overlap matrix elements $u, \sqrt{1-u^2}$, etc, in (5.6) give rise to factor similar to (5.12). Thus the rates read as

$$\Gamma_{lr'} \propto \frac{\Omega^2_{L'R'}}{\Omega^2_{L'R'} + \epsilon^2_{L'R'}} \Gamma_{l'l'} \tag{8.1}$$

where Ω is the off-diagonal matrix element. $\epsilon = g\mu B(L' - R')$ is the asymmetry induced by the magnetic field, and $\Gamma_{l'l'}$ is the level width of the quantum state l'. Thus in the limit where $B = 0$ and in the absence of a longitudinal hyperfine field, the rate for transitions from the left-hand well to the right-hand one is roughly identical to the level width; for large B the rate is proportional to $\Omega^2_{L'R'}/\epsilon^2_{L'R'}$.

Very recently, a related problem has been tackled perturbatively in terms of the angular momentum basis [23]; the resulting rate for transition between excited states reads in our notation

$$\Gamma \propto \frac{\Omega^2_{L'R'}}{\Gamma^2_{l'l'} + \epsilon^2_{L'R'}} \Gamma_{l'l'}. \tag{8.2}$$

Hence for zero field $B = 0$, i.e. $\epsilon = 0$, and small level width, $\Gamma_{l'l'} \ll \Omega_{L'R'}$, the relaxation rate is inversely proportional to the width, $\Gamma \propto 1/\Gamma_{l'l'}$, which is clearly unphysical. (For vanishing phonon coupling, one finds $\Gamma_{l'l'} \to 0$ and hence a diverging relaxation rate $\Gamma \to \infty$.) This problem arises since Ω^2 is missing in the denominator of (8.2).

Garanin and Chudnovsky studied the present problem using perturbation theory for the angular momentum states [21]. By mapping the relaxation between molecular states on a corresponding conductance problem, these authors perform implicitly a partial summation of the perturbation series and hence avoid the above shortcoming of the angular momentum basis.

Since it is based on energy eigenstates, the present approach does not encounter such a diverging energy denominator; in second order it already gives the correct result in the limit of zero field.

8.2. The nature of resonant transitions: the hybrid process

As a most striking feature, the relaxation rate shows resonances at those values for the magnetic field where the levels in the left-hand and right-hand wells cross. The origin of

these resonances may be traced back to the overlap matrix elements $v_{lr'}$ that are maximum where the offset due to the magnetic field and the hyperfine coupling vanishes.

Such a behaviour has been discussed before by several authors; e.g. in references [26, 13]. Note, however, an essential difference with respect to the nature of the microscopic process. It has been generally assumed that the system is scattered from the left-hand state l of such a resonant level pair to the right-hand one, r.

In view of our perturbation theory, it turns out that the most relevant process occurs between states that belong to *different* pairs; cf. the transition (2) in figure 2. We find that the phonon-assisted rate of transfer between resonant levels—in our notation $\Gamma_{\rm dir}$—is insignificant, except for very low temperatures and small B. For T not too small, the non-diagonal resonant transitions are more efficient, because of the strong frequency dependence of the bath spectral density $\varphi''(\omega)$.

Relaxation from the left-hand to the right-hand well involves a change of both *energy* and *magnetization*, thus requiring a *hybrid* process. Energy conservation is ensured by absorption or emission of a phonon, whereas the magnetization is carried away by the transverse hyperfine field h_x that is hidden in the off-diagonal entries Ω_{NM}. Accordingly, the rate is proportional to the square of the elastic deformation potential γ and to the square of the relevant Ω_{LR}. The former appears in the parameter α in (2.22), whereas the latter is hidden in the factor v^2 of the rate; equation (6.5) displays both factors most clearly.

8.3. Transition without phonons

The phonon-driven rate becomes very small in the limit of zero temperature and zero field, since it involves the phonon density of states at very low frequency. In this range the nuclear spins may act as a heat bath more efficiently than acoustic waves [24]. There is experimental evidence for this occurring for $T \to 0$, resulting in a constant rate that does not depend on phonon coupling [10].

8.4. Coherent motion between the two wells

The time propagator $\mathcal{U}$ derived in section 2 factorizes in two parts, $\mathcal{V}$ and $\mathcal{W}$ (cf. equations (2.12)–(2.17)). The former describes the relaxational, or zero-frequency, dynamics of the spin system; the resulting long-time behaviour of the magnetization is the main issue of this paper.

Here we briefly address the second part, $\mathcal{W}(t)$, that accounts for the oscillatory, or coherent, time evolution of the electron spins; it gives rise to damped oscillations in the experimentally relevant two-time correlation function $C(t - t') = \langle S_z(t) S_z(t') \rangle_\rho$. In a scattering experiment, the resolvent $\mathcal{W}(z)$ would describe inelastic transitions with resonance frequencies Δ_{nm} and widths τ_{nm}^{-1}.

The most interesting case concerns very low temperature and zero magnetic field. These conditions ensure that there is only a single resonance frequency, i.e., the ground-state splitting $\hbar\Delta = \sqrt{\Omega^2 + \epsilon^2}$. When calculating the oscillatory contribution to the correlation function, one finds, moreover, that it is reduced by a residue factor:

$$C_{\rm res}(t) = (\Omega^2/\hbar^2\Delta^2)\cos(\Delta t)\exp(-t/\tau). \tag{8.3}$$

As a consequence, the oscillations disappear as soon as the bias ϵ exceeds the tunnel energy Ω. The latter, however, is smaller by many orders of magnitude than the random hyperfine field h_z, thus rendering hopeless the search for those oscillations. But even if one could detect a signal as weak as $\Omega^2/\hbar^2\Delta^2$, the average over h_z would result in a broad distribution

of frequencies, since $\hbar\Delta = \sqrt{\Omega^2 + S^2 h_z^2}$ for $B = 0$. As a further complication, one finds that phonon damping is strong, resulting in a phase coherence time τ that reaches the millisecond range only at *very* low T; it is much shorter than the barrier crossing time $1/\Gamma_\downarrow$.

From this discussion we conclude that both nuclear spins and phonons would destroy the coherent motion of S_z, due to the small energy overlap Ω of the ground states in the two wells. In this sense, the twelve spins of $Mn_{12}Ac$ are already too large a system to show quantum coherence.

9. Summary

In this paper we have investigated the relaxation behaviour of mesoscopic molecules such as $Mn_{12}Ac$. We have explicitly evaluated the reduced spin propagator, by expanding the self-energy matrix in terms of the spin–phonon coupling. The dynamics occurs on two very different timescales that are given by the rate for transitions within one well, and the rate for transitions from one well to the other. Since the latter one is much smaller, magnetic relaxation may be reduced to an effective two-state problem. Here we summarize our main results.

(i) The most relevant phonon-mediated transitions do not occur between almost degenerate levels, but from one resonant pair to another; compare (2) in figure 2.

(ii) The relaxation rate is strongly enhanced at the 'resonant' values of the magnetic field (1.2), with $J = 0, 1, 2, \ldots$. The width of these resonances is determined by the longitudinal hyperfine field b_z.

(iii) The resonances are not symmetric about B_J, but slightly shifted to positive $B - B_J$. This effect arises from the fact that a small excess field lowers the activation energy for non-diagonal resonances. Compare this with figure 4.

(iv) At temperatures above 2 K, transitions close to the top of the barrier are the most efficient; as a consequence, the rate shows activated behaviour where $V = S^2 A - g\mu SB$ is given by the energy distance from the ground state in the left-hand well to the top of the barrier.

(v) Below about 1 K and for sufficiently large magnetic field, $g\mu B \geqslant A$, the rate is constant as a function of temperature. For small field, $g\mu B \ll A$, it shows Arrhenius behaviour with the activation energy $V = (2S - 1)A$.

(vi) At very low temperature, the rate is determined by the direct phonon process in the ground-state doublet. For small field, $g\mu B \ll A$, and $T = 0$, relaxation is *very* slow, with a rate that is linear in B. At small field and small but finite temperature, the rate varies linearly with T and is independent of B; cf. equations (6.5) and (6.6). As a consequence, the rate for direct transitions is significantly smaller than those discussed in previous work; this rate is reduced by a factor $\Omega^2/[\Omega^2 + (2Sg\mu B)^2]$, which may be much smaller than unity. See the discussion below equations (5.14) and (7.2).

Acknowledgment

Valuable discussions with Jacques Villain are gratefully acknowledged.

References

[1] Gunther L and Barbara B (ed) 1995 *Quantum Tunneling of Magnetization (NATO ASI Series E)* (Dordrecht: Kluwer)

[2] Barbara B, Sampaio L C, Wegrowe J E, Ratman B A, Marchand A, Paulsen C, Novak M A, Tholence J L, Uehara M and Fruchart D 1993 *J. Appl. Phys.* **73** 6703

[3] Stamp P C E 1991 *Phys. Rev. Lett.* **66** 2802
Stamp P C E 1992 *Nature* **359** 365

[4] Enz M and Schilling R 1986 *J. Phys. C: Solid State Phys.* **19** 711

[5] Van Hemmen J L and Sütő A 1986 *Europhys. Lett.* **1** 481
Van Hemmen J L and Sütő A 1986 *Physica* B **141** 37

[6] Chudnovsky E M and Gunther L 1988 *Phys. Rev. Lett.* **60** 661

[7] Garanin D A 1991 *J. Phys. A: Math. Gen.* **24** L61

[8] Chudnovsky E 1993 *J. Appl. Phys.* **73** 6697

[9] Sessoli R, Gatteschi D, Caneschi A and Novak M A 1993 *Nature* **365** 141
Sessoli R *et al* 1993 *J. Am. Chem. Soc.* **115** 1804

[10] Paulsen C and Park J-G 1995 *Quantum Tunneling of Magnetization (NATO ASI Series E)* ed L Gunther and B Barbara (Dordrecht: Kluwer) p 187

[11] Sangregorio, C, Ohm T, Paulsen C, Sessoli R and Gatteschi D 1997 *Phys. Rev. Lett.* **78** 4645

[12] Hernandez J M, Zhang X X, Luis F, Bartolomé J, Tejada J and Ziolo R 1996 *Europhys. Lett.* **35** 301

[13] Hernandez J M, Zhang X X, Luis F, Tejada J, Friedmann J R, Sarachik M P and Ziolo R 1997 *Phys. Rev.* B **55** 5858

[14] Barbara B, Wernsdorfer W, Sampaio L C, Park J G, Paulsen C, Novak M A, Ferré R, Mailly D, Sessoli R, Caneschi A, Hasselbach K, Benoit A and Thomas L 1995 *J. Magn. Magn. Mater.* **140–144** 1825

[15] Thomas L, Lionti F, Ballou R, Gatteschi D, Sessoli R and Barbara B 1996 *Nature* **383** 145

[16] Barbara B, Thomas L, Lionti F, Sulpice A and Caneschi A 1997 *Preprint*

[17] Politi P, Rettori A, Hartmann-Boutron F and Villain J 1995 *Phys. Rev. Lett.* **75** 537

[18] Garg A and Kim G-H 1989 *Phys. Rev. Lett.* **63** 2512

[19] Villain J, Hartmann-Boutron F, Sessoli R and Rettori A 1994 *Europhys. Lett.* **27** 301

[20] Villain J, Würger A, Fort A and Rettori A 1997 *J. Physique* I **7** 1583

[21] Garanin D A and Chudnovsky E M 1997 *Phys. Rev.* B **56** 11 102

[22] Luis F, Bartolomé J and Fernández J F 1998 *Phys. Rev.* B **57** 505

[23] Fort A, Rettori A, Villain J, Gatteschi D and Sessoli R 1998 *Phys. Rev. Lett.* **80** 612

[24] Burin A L, Prokof'ev N V and Stamp P C E 1996 *Phys. Rev. Lett.* **76** C3040

[25] Prokof'ev N V and Stamp P C E 1995 *Quantum Tunneling of Magnetization (NATO ASI Series E)* ed L Gunther and B Barbara (Dordrecht: Kluwer)

[26] Hartmann-Boutron F, Politi P and Villain J 1996 *Int. J. Mod. Phys.* **10** 2577

[27] Nakajima S 1958 *Prog. Theor. Phys.* **20** 948

[28] Zwanzig R 1960 *J. Chem. Phys.* **33** 1338

[29] Haake F 1973 *Statistical Treatment of Open Systems by Generalized Master Equations (Springer Tracts in Modern Physics 66)* (Berlin: Springer)

[30] Würger A 1989 *Z. Phys.* B **76** 65

[31] Würger A 1998 *Phys. Rev.* B **57** 347

[32] Abragam A and Bleaney B 1970 *Electron Paramagnetic Resonance of Transition Ions* (Oxford: Clarendon)